Astronomy & Astrophysics

HCN(1–0) enhancement in the bar of NGC 2903

S. Leon[1], S. Jeyakumar[2], D. Pérez-Ramírez[3], L. Verdes-Montenegro[4], S. W. Lee[5], and B. Ocaña Flaquer[1]

[1] Instituto de Radioastronomía Milimétrica (IRAM), Avenida Divina Pastora 7, Núcleo Central, 18012 Granada, Spain
e-mail: leon@iram.es
[2] Departamento de AstronomÃŋa, Universidad de Guanajuato, AP 144, Guanajuato CP 36000, Mexico
[3] University of Jaén, Jaén, Spain
[4] Instituto de Astrofísica de Andalucía-CSIC, Granada, Spain
[5] University of Toronto, Astronomy Department, Toronto, Canada

ABSTRACT

We have mapped the HCN(1–0) emission from two spiral galaxies, NGC 2903 and NGC 3504 to study the gas properties in the bars. The HCN(1–0) emission is detected in the center and along the bar of NGC 2903. The line ratio HCN(1–0)/^{12}CO(1–0) ranges from 0.07 to 0.12 with the lowest value in the center. The enhancement of HCN(1–0) emission along the bar indicates a higher fraction of dense molecular gas in the bar than at the center. The mass of dense molecular gas in the center ($2.2 \times 10^7 \ \mathcal{M}_\odot$) is about 6 times lower than that in the bar ($1.2 \times 10^8 \ \mathcal{M}_\odot$). The total star formation rate (SFR) is estimated to be 1.4 $\mathcal{M}_\odot$ yr^{-1}, where the SFR at the center is 1.9 times higher than that in the bar. The time scale of consumption of the dense molecular gas in the center is about $\sim 3 \times 10^7$ yr which is much shorter than that in the bar of about 2 to 10×10^8 yr. The dynamical time scale of inflow of the gas from the bar to the center is shorter than the consumption time scale in the bar, which suggests that the star formation (SF) activity at the center is not deprived of fuel. In the bar, the fraction of dense molecular gas mass relative to the total molecular gas mass is twice as high along the leading edge than along the central axis of the bar. The HCN(1–0) emission has a large velocity dispersion in the bar, which can be attributed partially to the streaming motions indicative of shocks along the bar. In NGC 3504, the HCN(1–0) emission is detected only at the center. The fraction of dense molecular gas mass in the center is about 15%. Comparison of the SFR with the predictions from numerical simulations suggest that NGC 2903 harbors a young type B bar with a strong inflow of gas toward the center whereas NGC 3504 has an older bar and has already passed the phase of inflow of gas toward the center.

Key words. galaxies: spiral – galaxies: ISM – galaxies: evolution

1. Introduction

The molecular interstellar medium in galaxies has been extensively studied through the rotational transitions of CO at millimeter wavelengths. These transitions are good tracers of the molecular gas mass and represent the general distribution of molecular hydrogen (e.g. Young & Scoville 1982; Young & Devereux 1991). High-density gas tracer molecules, like HCN, add relevant information to this view concerning the dense gas ($n_{H_2} > 10^4$ cm^{-3}). Observational evidence (Nguyen et al. 1992; Reynaud & Downes 1997; Kohno et al. 1999a) has suggested a close relationship between dense molecular gas and massive star formation in the centers of galaxies. In the center of the starburst galaxies, the HCN line emission is tightly correlated with the radio-continuum emission (see e.g. in NGC 1530, Reynaud & Downes 1997) and the total HCN luminosity correlates with the far-infrared (FIR) luminosity (Solomon et al. 1992; Gao & Solomon 2004), although contradictory results have been found, e.g. by Aalto et al. (1995). Since only very few galaxies have been mapped in HCN line emission at large scales, this correlation remains a source of speculation, especially for milder star formation (SF), typically 2 $\mathcal{M}_\odot$ yr^{-1} or less.

The SF in the center0s of galaxies and in the spiral arms has been extensively studied. Nevertheless the processes involved in the SF activity in the bar itself are still not well understood. Hydrodynamical and N-body simulations show inflow of gas along the leading edge after a shock, losing angular momentum (Athanassoula 1992). Sticky particle simulations of the gas in

barred galaxies (Combes & Gerin 1985) produce the same configuration of enhanced molecular gas along the leading edge due to crossing/crowding of orbits. The role of gas orbits in a barred potential on the star formation activity is still poorly understood.

Various observational studies using CO emission have found that molecular gas is located mainly along the leading edge of the bars (e.g. Handa et al. 1990; Reynaud & Downes 1997; Downes et al. 1996; Sheth et al. 2002). However a contribution from large scale diffuse, unbound gas in the bar of the galaxy NGC 7479 has been suggested by Hüttemeister et al. (2000).

In the bar of NGC 1530, Reynaud & Downes (1998) have detected large velocity gradients due to velocity jumps between the upstream regions and the shock along the leading edge. These shocks would inhibit the SF by destroying the giant molecular clouds because of a large shear.

The CO line is a tracer of molecular gas at low densities, whereas star formation occurs in very dense molecular clouds (Solomon et al. 1992; Paglione et al. 1995; Hatchell et al. 1998) which can be traced by the HCN transitions. To study the formation of dense molecular gas and its relation to SF, the bars offer an unique dynamical system to analyse the effects of a strong density wave on the molecular gas and SF. Moreover, numerical simulations and Hα observations (Martin & Friedli 1997; Verley et al. 2007) have shown a tight correlation between the SF along the bars and the age of the bars, which suggests that a similar correlation can be expected for the HCN(1–0) emission in the bar because of the tight relationship between the SF and the dense molecular gas.

Table 1. The basic parameters of the galaxies.

	NGC 2903	NGC 3504
α_{2000}	$09^h32^m09.9^s$	$11^h03^m11.21^s$
δ_{2000}	$+21^d31^m01^s$	$+27^d58^m21.0^s$
Type[a]	SB(s)d	(R)SAB(s)ab
V_{lsr} (km s^{-1})	560	1534
Distance (Mpc)	8.6[b]	20[c]
m_B^a	9.59	11.69
PA	17°[d]	149°[c]
Bar PA	20°[d]	143°[c]
L_{FIR}^a ($10^9\ L_\odot$)	8.8	14.3
$M(H_2)$ ($10^9\ \mathcal{M}_\odot$)	1.2[e]	1.4[e]
SFR^f ($\mathcal{M}_\odot$ yr^{-1})	1.5	2.5

[a] From NED. [b] Telesco & Harper (1980). [c] Kenney et al. (1993). [d] Sheth et al. (2002). [e] This paper. [f] Kennicutt (1998)

In this paper we present the result of the HCN observations at the IRAM-30 m telescope, along the bars of two spiral galaxies which have been chosen for their previous detection of HCN in the center. In Sect. 2, the IRAM observations are described. The main results of the NGC 3504 and NGC 2903 observations are presented in Sects. 3 and 4 respectively. The SF activity is discussed in Sect. 5 and a discussion about the molecular gas properties in the bar is presented in Sect. 6.

2. Observations

During May and August 2002, we observed two barred galaxies, namely NGC 2903 and NGC 3504, using the IRAM-30 m telescope. NGC 2903 and NGC 3504 were observed in good weather conditions. The basic parameters of the NGC 2903 and NGC 3504 are given in the Table 1. The main goal was to map the HCN(1–0) emission along the bar of each galaxy. Given the beam size at 88 GHz (27″) and the width of the bar (~48″, see below) for both galaxies, the maps were obtained with a sampling of 20″ along the bar and ±20″ perpendicular to the bar axis to sample the leading/trailing edge as well. The ^{12}CO(2–1) line was observed in parallel, with a spatial resolution of 10″ but spatially undersampled with the 20″ sampling and they are not presented in this paper, except for the central point in Fig. 3. NGC 3504 was mapped along the bar with a larger coverture on the Southeast side up to a radius of 50″ in the bar frame. NGC 2903 was mapped in HCN(1–0) along the bar (PA = 20°) and along both sides of the bar (±20″ in the bar frame). The individual target positions are shown in Fig. 1. To measure the HCN(1–0) on the trailing/leading edge of the bar we mapped from 10″ to 70″ (2.9 kpc) on the northern side of the bar, with an offset of ±20″ perpendicular to the bar axis and a sampling of 20″. The *FWHM* of the bar structure, estimated using the *J*-band image of the Two Micron All Sky Survey, measured at 30″ from the center after a rotation by –20°, is about 48″ (see Fig. 2). For this size of the bar, the pointings at ±20″ offsets along the bar cover the trailing and leading edge of the bar respectively.

The spectrometer used for the observations of the HCN(1–0) line was the filterbank (512 × 1 MHz channels) and for the ^{12}CO(2–1) line an autocorrelator (409 × 1.25 MHz resolution) was used. For the HCN(1–0) observations the typical rms noise temperature is about 4 mK (T_a^* scale) at a velocity resolution of 3.4 km s^{-1}. After subtracting a polynomial baseline of order at most 1, the spectra were smoothed by the Hanning convolution to obtain a velocity resolution of 27 km s^{-1} with an rms temperature of 1 mK and 5 mK for the observations of NGC 2903

and NGC 3504 respectively. Pointing observations on a strong radio source close to the galaxies were performed every 90 min with good accuracy, and the expected rms error on the pointing is ~3″ which is about 10% of the beam size at the frequency of the HCN(1–0) transition.

3. HCN(1–0) emission in NGC 3504

We detected HCN(1–0) emission only at the center (0″, 0″) and at the offset position (12″, –16″), i.e. (20″, 0″) in the bar frame (see Fig. 3). Here the positive offsets represent the northern side. Observed line parameters are listed for these two positions in Table 2. No HCN(1–0) emission was detected at other positions along the bar (PA = 143°), from –60 to 60″ in steps of 20″ in the bar frame and at 10″, 30″, 50″, 70″ with ±20″ offset perpendicular to the bar, for a typical rms noise temperature of 1.5–2 mK at a velocity resolution of 13.6 km s^{-1}. Previous interferometric maps of NGC 3504 by Kohno et al. (1999a) also reveal a central concentration of HCN(1–0) emission, with a high surface density of molecular gas.

The ratio of the integrated line intensity of HCN(1–0) to that of the ^{12}CO(1–0), $\mathfrak{R}_{HCN/CO}$, is an indicator of the molecular gas density and temperature (Kohno et al. 1999b). Using the ^{12}CO(1–0) integrated intensity of 7.55 K km s^{-1} at the center, detected with the FCRAO 14 m telescope (Young et al. 1995) the ratio $\mathfrak{R}_{HCN/CO}$ is estimated to be about 0.12. However this ratio is an underestimate since the FCRAO 14 m beam size of (45″) at the ^{12}CO(1–0) frequency is larger than the IRAM-30 m beam size (27″) at the HCN(1–0) frequency. Because of the undersampling of the ^{12}CO(2–1) IRAM-30 m pointing we were not able to constrain the source size using these data. Indeed with interferometric observations, Kohno et al. (1999a) found a line ratio $\mathfrak{R}_{HCN/CO}$ of 0.3 in the center of the galaxy which is consistent with our value if the beam dilution factor is taken into account (about 2.8) assuming that the central HCN and CO emission is unresolved.

If HCN is tracing the dense phase of the molecular gas, the mass of the dense molecular gas can be estimated from the HCN(1–0) integrated intensity. Following Gao & Solomon (2004) we use the relation,

$$M_{HCN}(H_2) \approx 10 \times L_{HCN}\ \mathcal{M}_\odot\ (\text{K km s}^{-1}\ \text{pc}^2)^{-1}$$

to estimate the dense molecular gas mass from the HCN luminosity (L_{HCN}). The HCN luminosity in the area covered by the IRAM beam size is estimated to be 2.1×10^7 K km s^{-1} pc^2 which gives a molecular mass of $M_{HCN}(H_2) \approx 2.1 \times 10^8\ \mathcal{M}_\odot$. The molecular gas mass $M(H_2)$ is estimated using the standard CO-to-H$_2$ conversion factor (Young et al. 1996),

$$M(H_2) = 1.1 \times 10^4 D^2 S_{CO}$$

where D is the is the distance (Mpc) and S_{CO} is the ^{12}CO(1–0) integrated intensity (Jy km s^{-1}), obtained from Young et al. (1995). Thus the molecular gas mass in the central 45″ is estimated to be about $1.4 \times 10^9\ \mathcal{M}_\odot$.

The dense molecular gas traced by HCN is about 15% of the total molecular gas in the center of NGC 3504. Moreover, high spatial resolution ^{12}CO(1–0) imaging from the IRAM Plateau de Bure Interferometer indicates that the molecular gas is concentrated in the inner 10″ of the galaxy. Thus, NGC 3504 has the high concentration of dense molecular gas necessary to feed its central starburst.
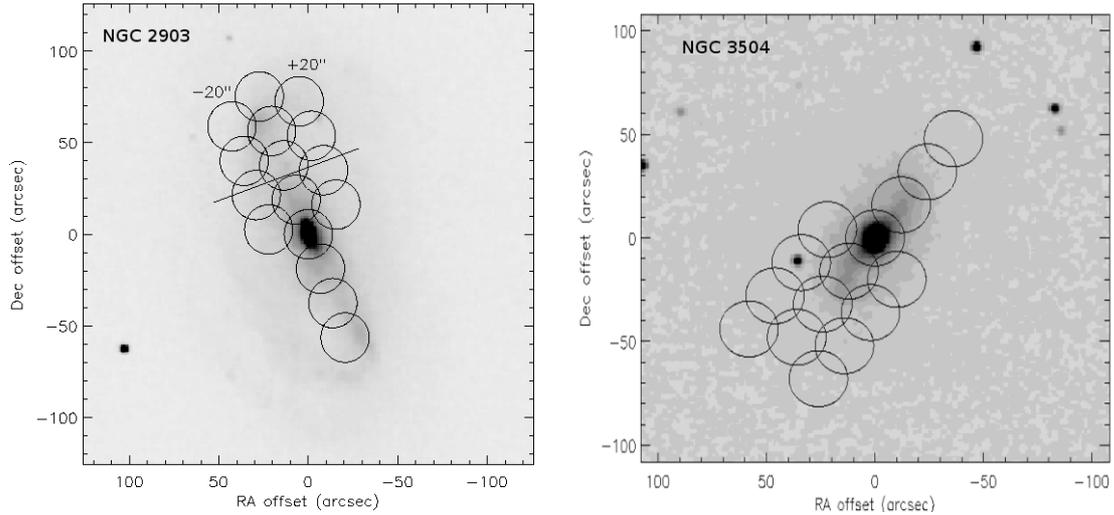
Fig. 1. The positions in NGC 2903 and NGC 3504 of HCN pointing are shown as circles of the size of the beam (27″) overlaid on the 2MASS *J* band image. The offsets –20″ and +20″ in NGC 2903 indicate the leading and trailing edge of the bar. The solid line indicates the cut across which the width of the bar is estimated (see Fig. 2).
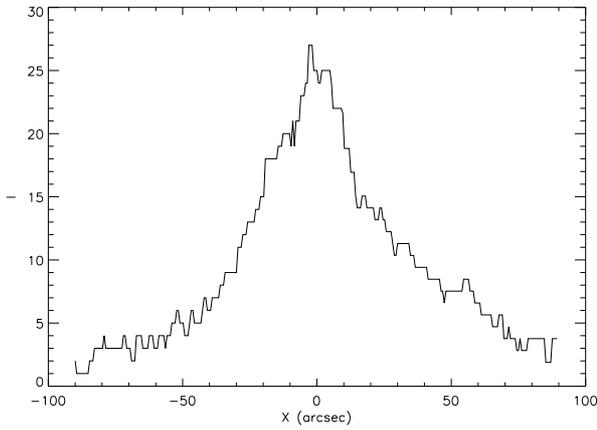

Fig. 2. *J*-band intensity from 2MASS data (arbitrary units) across the cut perpendicular to the bar PA in NGC 2903, at a distance of 30″ from the center. The *FWHM* is estimated to be 48″.

4. HCN(1–0) in NGC 2903

4.1. HCN(1–0) distribution

HCN(1–0) emission is detected along the central bar axis of NGC 2903 out to a radius of 60″. The observed intensities for all the pointing positions are given in Table 3. Toward the center we detect a line intensity of 1.36 K km s^{-1}, which is about 2.7 times greater than the value obtained by Helfer & Blitz (1993) using the NRAO-12 m telescope with a beam size of 63″. This is likely due to the beam dilution effect.

On the northern side, the HCN(1–0) emission is detected mainly from the central axis and the leading edge of the bar (see Fig. 4). At a similar rms noise temperature of about 1.5–2 mK, there is no detection on the trailing edge at the offsets (30″, 20″), (50″, 20″) and (70″, 20″). However the only detection of HCN(10) at positive offsets from the bar axis. i.e. (10″, 20″), correlates with the CO extension from the center observed by Sheth et al. (2002). Figure 5 shows the radial distribution of the integrated intensity of the HCN(1–0) line along the bar. Besides the strong central emission, there is no radial trend for the HCN(1–0) emission along the bar. The integrated intensity of HCN(1–0) along the axis of the bar ranging from 0.7 to
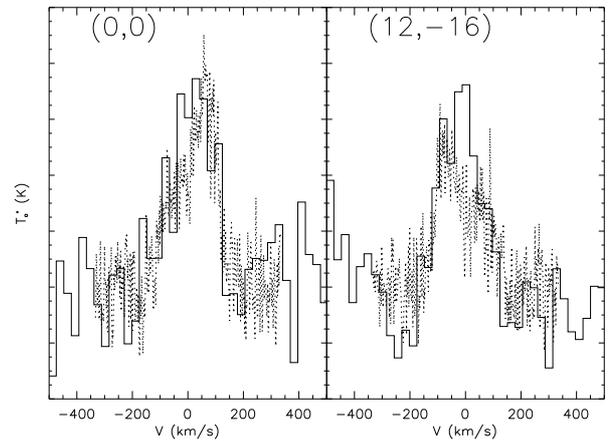

Fig. 3. The HCN(1–0) (solid line) and ^{12}CO(2–1) (dotted line) spectra shown for the offset positions (0″, 0″) and (12″, –16″) in the galaxy NGC 3504. The ^{12}CO(2–1) intensity is scaled down by a factor of 20 for comparison.

Table 2. Observed properties of HCN(1–0) emission in NGC 3504.

X offset (″)	Y offset (″)	I (HCN(1–0)) K km s^{-1}	Velocity km s^{-1}	Width km s^{-1}
0	0	1.24	19	159.
12	–16	1.12	–21	149.

1 K km s^{-1} is slightly higher than that along the leading edge of the bar ranging from 0.3 to 0.7 K km s^{-1}.

The HCN(1–0) emission from the leading edge of the bar cannot be associated with the spiral arm, since the strong spiral arm emerging from the tip of the bar is located north of the trailing edge.

In Fig. 6, the 12CO(10) integrated intensity from the BIMA Survey Of Nearby Galaxies is shown together with the HCN(1–0) pointings as circles. The beam size at the HCN(1–0) frequency and the sampling in the direction perpendicular to the bar axis does not allow us to clearly distinguish the origin of the HCN(1–0) emission between the central axis and the edges of the bar. Nevertheless, detection of HCN(1–0) on the leading
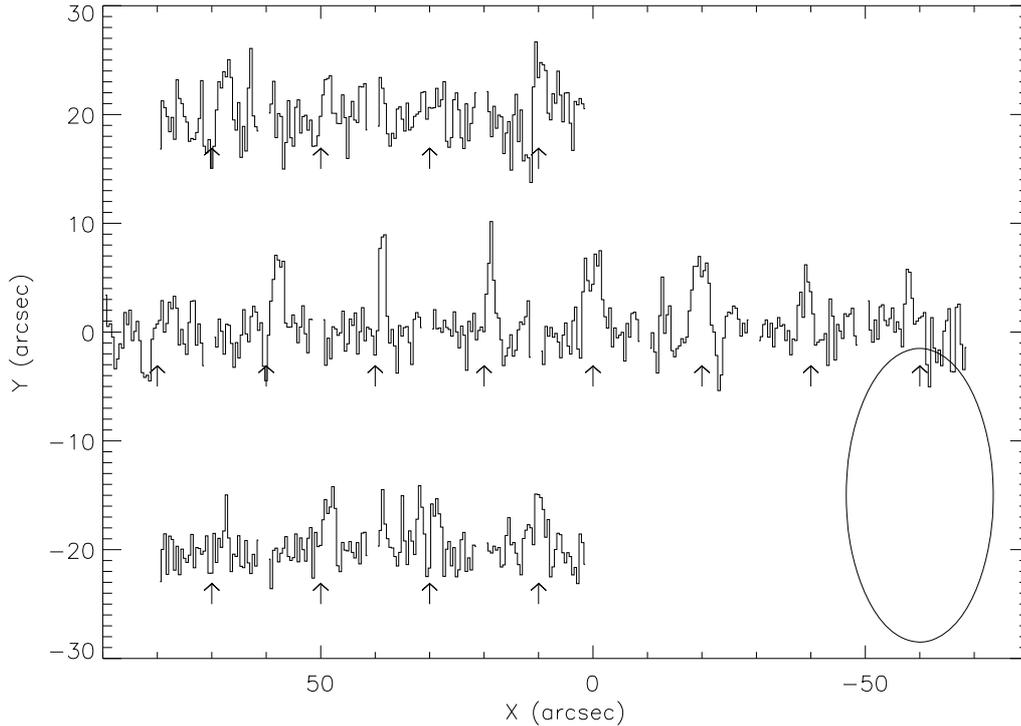
Fig. 4. The HCN(1–0) spectra along the bar of NGC 2903 for each pointing. The positions are in the frame of the bar. The width of each spectrum ranges from –571 to 567 km s^{-1} relative to the systemic velocity of the galaxy with a velocity resolution of 27 km s^{-1} and the LSR velocity is marked with arrows. The bar axis corresponds to the x-axis. The beam size at the HCN(1–0) frequency is indicated by the ellipse in *the bottom right corner.*

Table 3. Observed properties of HCN(1–0) emission along the bar of NGC 2903. The offset positions X and Y are in the frame of the bar. The positive X offsets refer to the northern side of the bar. The error (σ) in I(HCN(1–0)) is given between parentheses.

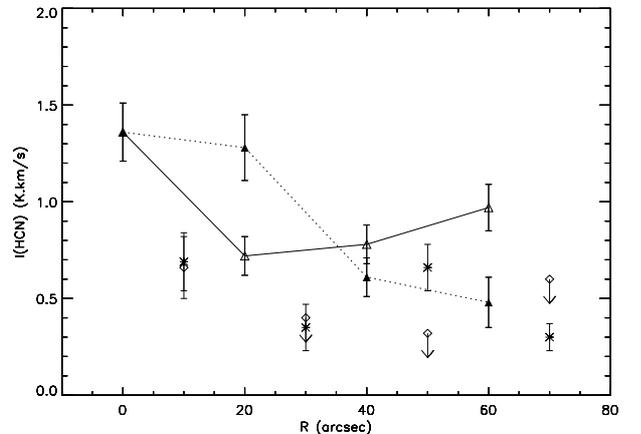| X ('')	Y ('')	I_{HCN} K km s^{-1}	Central velocity km s^{-1}	Width km s^{-1}	$M_{HCN}(H_2)$ $\mathcal{M}_\odot$
0	0	1.36 (0.15)	–23.	200.	2.2×10^7
20	0	0.72 (0.10)	–74.	69.	1.2×10^7
40	0	0.78 (0.10)	–84	66.	1.3×10^7
60	0	0.97 (0.12)	–134	118	1.6×10^7
80	0	<0.40			$<6.6 \times 10^6$
–20	0	1.28 (0.17)	19.	167	2.1×10^7
–40	0	0.61 (0.10)	48	111	1.0×10^7
–60	0	0.48 (0.13)	121	69	8.0×10^6
10	20	0.66 (0.16)	–21	109	1.1×10^7
10	–20	0.69 (0.15)	–4	128	1.1×10^7
30	20	<0.40			$<6.6 \times 10^6$
30	–20	0.35 (0.12)	–73	79	5.8×10^6
50	20	<0.32			$<5.3 \times 10^6$
50	–20	0.66 (0.12)	–96	122	1.1×10^7
70	20	<0.60			$<10^7$
70	–20	0.30 (0.07)	–159	40.	5.0×10^6

Fig. 5. The integrated intensity of HCN(1–0) along the northern side of the bar in NGC 2903 against the offset from the center measured in the frame of the bar. The triangles represent the axial positions in the bar (open symbols: northern side, filled symbols: southern side), the asterisks represent the leading edge positions (–20'' vertically from the axis of the bar) and the diamonds represent the trailing edge positions (20'' vertically from the axis of the bar). The upper limits for the trailing edge positions are indicated by a diamond with a downward arrow, taking the velocity width at the same radius in the central part of the bar.

side of the bar indicates that the HCN(1–0) emission is either spatially correlated or downstream of the ^{12}CO(1–0) emission.

4.2. HCN(1–0)/CO(1–0) line ratio

As a first estimate, the ratio, $\mathfrak{R}_{HCN/CO}$, is computed using the ^{12}CO(1–0) integrated intensity of 13.16 K km s^{-1} observed towards the center with the FCRAO-14 m telescope (Young et al. 1995). The ratio $\mathfrak{R}_{HCN/CO}$ at the center is 0.074 which is

probably an underestimate as in the case of NGC 3504, due to different beam sizes. Young et al. (1995) have mapped the bar of NGC 2903 in CO. We used their observation at the offset (13'', 43'') in RA, Dec coordinates and estimated the ratio, $\mathfrak{R}_{HCN/CO}$, to be about 0.13 at the offset (40, 0) in the bar frame. This is about twice the size of that at the center. However, their observations are offset by (0.7'', 5.4'') relative to our pointing and their beam size is about 20% larger.
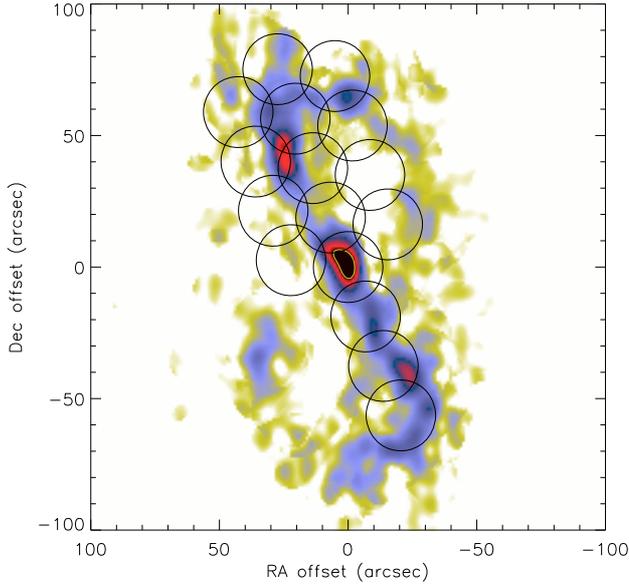
Fig. 6. The positions of HCN pointing shown as circles of the size of the beam (27″) is overlaid on the gray scale image of the integrated intensity of ^{12}CO(1–0) emission reproduced from the BIMA SONG survey by Helfer et al. (2003).
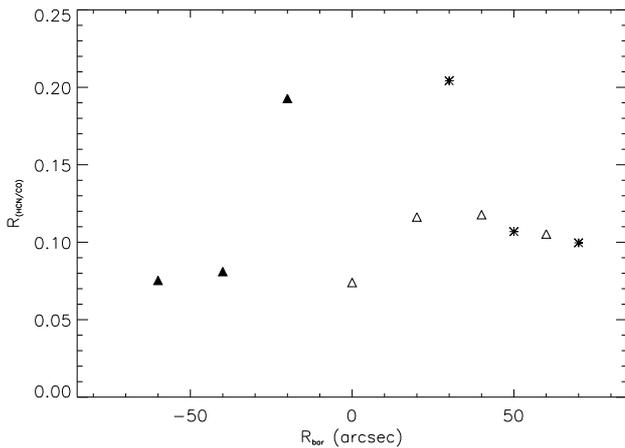

Fig. 7. $\Re_{HCN/CO}$ ratio computed using the CO data from BIMA-SONG observations (Helfer et al. 2003) and HCN(1–0) from the current observations against the offset measured in the frame of the bar. The symbols have the same meaning as in Fig. 5.

Since we have no IRAM-30 m single dish ^{12}CO(1–0) observations for any of the offsets, we used the interferometric observation from the BIMA-SONG survey (Helfer et al. 2003) to obtain a more accurate estimate of $\Re_{HCN/CO}$. These interferometric observations have also been combined with single dish observations from the NRAO-12 m telescope and therefore there is no missing flux of the large scale ^{12}CO(1–0) emission (Sheth et al. 2002). The ratio for all the positions are shown in Fig. 7. The ratio in the bar ranges from 0.07 to 0.12 without any trend with respect to the perpendicular offsets. Nevertheless a slight drop of the ratio is noticeable along the bar. The line ratio on the northern side ranging from 0.09 to 0.12 is larger than that on the southern side of ~0.07. This asymmetry in the line ratio between the northern and the southern sides of the bar is probably due to asymmetric physical conditions of the gas in the bar. Such asymmetry is seen in another barred galaxy, NGC 7479 (Huttemeister et al. 2000), where more diffuse gas is present on one side.

Table 4. The mass of the molecular gas traced by the HCN(1–0) and ^{12}CO(1–0) emission are listed in the bar of NGC 2903. The total mass is estimated by summing all the positions along the axis, leading and trailing edges seperately, excluding the central position. Between parentheses we give the 1σ error.

Bar location	$M_{HCN}(H_2)$ $(10^7\,\mathcal{M}_\odot)$	$M_{CO}(H_2)$ $(10^7\,\mathcal{M}_\odot)$	$\frac{M_{HCN}(H_2)}{M_{CO}(H_2)}$
Central axis (North)	4.1 (0.8)	62.1 (0.1)	6.6%
Central axis (South)	3.9 (0.7)	49.4 (0.2)	7.9%
Leading edge	3.3 (0.8)	29.8 (0.2)	11.0%
Trailing edge	1.1 (0.3)	20.6 (0.2)	5.3%

On the leading edge of the northern side, at the offset +30″ in the bar frame, a ratio of ~0.20 is found. But given the sharp decrease of CO at the edge of the 30 m beam at the HCN(1–0) frequency, it may be attributed to a pointing offset relative to the interferometric map. Similarly the ratio found at the offset +10″ on the trailing and leading edges of the bar is very high (~0.5) and similarly could be due to a slight offset of the HCN(1–0) pointings towards the center. They are not displayed in the Fig. 7.

4.3. Dense molecular gas mass

The total molecular gas mass in NGC 2903 is estimated with the BIMA-SONG ^{12}CO(1–0) emission map as $1.2 \times 10^9\ \mathcal{M}_\odot$. All masses based on ^{12}CO(1–0) are calculated using the standard conversion factor. Following a similar procedure as for NGC 3504, we computed the mass of the dense molecular gas, $M_{HCN}(H_2)$, for all the pointings listed in Table 3. At the center, $M_{HCN}(H_2)$ is $2.2 \times 10^7\ \mathcal{M}_\odot$ whereas the total molecular gas mass is $4.4 \times 10^8 \mathcal{M}_\odot$ as computed from the ^{12}CO(1–0) integrated intensity using the BIMA-SONG map. About 3% of the molecular gas in the center is present in dense clumps. The mass of the dense molecular gas integrated over the HCN(1–0) pointings along the bar, excluding the central pointing, is $\sim 1.2 \times 10^8 \mathcal{M}_\odot$ which is about 7.5% of the total molecular gas mass of $1.6 \times 10^9 \mathcal{M}_\odot$ over the same area in the ^{12}CO(1–0) BIMA-SONG map. It indicates clearly that the formation of dense molecular gas in the bar is more efficient than in the center.

Omitting the southern side of the bar, since we did not observe the leading/trailing edge, we computed the dense molecular gas mass and the ratio to the total molecular gas mass for the offsets along the bar axis and the trailing and leading edges. As shown in Table 4 the fraction of dense gas is much higher in the leading edge than along the bar axis. The value computed for the trailing edge is dominated by the only detection at the offset (10″, 20″) close to the center. For the leading edge, the HCN(1–0) pointing close to the center represents 30% of the total gas mass along the leading edge in the bar. The fraction of dense gas mass along the leading edge is two times higher than that along the central axis, within the limitation of the spatial resolution of the HCN(1–0) observations. The bar of NGC 2903 is very different to that of NGC 7479, which is also classified as a type-B barred galaxy according to the nomemclature of Martin & Friedli (1997), where Huttemeister et al. (2000) detected HCN(1–0) emission only in the center.

4.4. Dynamics

Since the bar position angle (20°) is only slightly offset from the galaxy position angle (17°), the velocity along the bar is a good approximation for the rotation curve, if one neglects
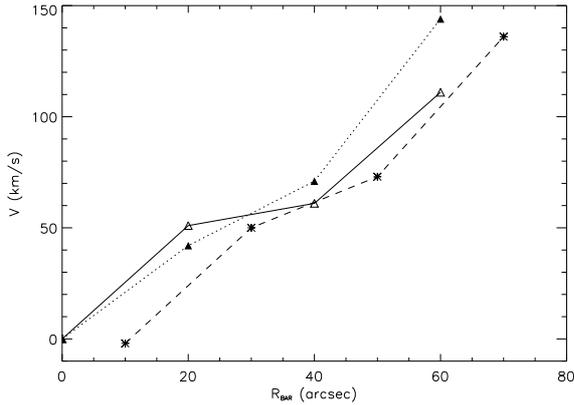
Fig. 8. The modulus of the velocity offset of HCN(1–0) emission along the bar relative to the systemic velocity of NGC 2903 against the offset measured in the axis of the frame. The symbols have the same meaning as in Fig. 5.
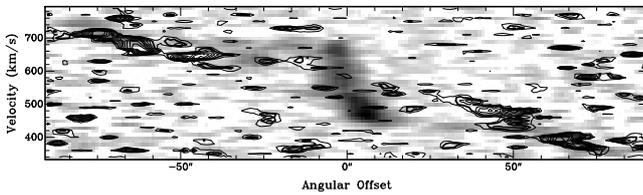

Fig. 9. Position velocity diagram (*p-v*) of the ^{12}CO(1–0) emission line from the BIMA-SONG map along the bar axis (greyscale) and along the northern leading side with positive radii and southern trailing side with negative radii (contours). The offset for the leading/trailing *p-v* diagram is $-20''$ relative to the bar axis. The velocities are in the local standard of rest frame.

any streaming motion along the bar. The velocity differences between the leading and trailing edges (see Fig. 8) and the ^{12}CO(1–0) position-velocity (*p-v*) diagram (see Fig. 9) from the BIMA-SONG suggest possible streaming motion of 50–80 km s^{-1}. For each offset position of the HCN(1–0) emission, the line of sight velocity and the velocity width are computed by fitting a Gaussian to the spectra.

An offset of 23 km s^{-1} is applied to the observed velocity to symmetrize the velocities of the receding and approaching sides of the bar. Thus the heliocentric systemic velocity of NGC 2903 is estimated to be 579 km s^{-1}. The projected rotation curve shown in Fig. 8 is close to symmetric, except at the radius of 60″ where there is a difference of 33 km s^{-1} between the approaching and receding side. The HCN(1–0) velocity in the leading edge of the approaching side is systematically lower than the bar axis velocity by 5–20 km s^{-1}. To analyze this velocity offset, the *p-v* diagram of the ^{12}CO(1–0) line from the BIMA-SONG map is computed along the bar axis and the northern leading edge (see Fig. 9). The velocity gradient is steeper along the leading edge (positive radii) than the trailing edge which may indicate that the CO-traced molecular gas is experiencing streaming motion along the leading edge (Athanassoula 1992). Indeed the shocks along the bar can create a velocity gradient as large as 100–200 km s^{-1} (Athanassoula 1992; Reynaud & Downes 1997). This result is confirmed by analyzing the *p-v* diagram on the southern leading edge which exhibits an even steeper gradient on the leading edge.

The velocity dispersion of the HCN(1–0) spectra detected along the bar is shown in Fig. 10. The velocity dispersion of HCN(1–0) is about 200 km s^{-1} in the center. Along the bar the velocity dispersion drops to 40–120 km s^{-1}, except for the
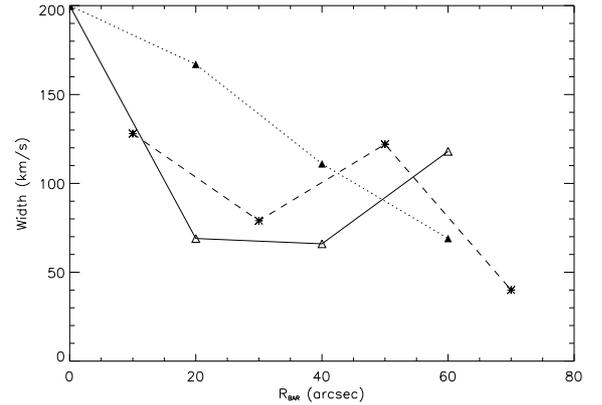

Fig. 10. The velocity dispersion of HCN(1–0) emission along the bar of NGC 2903 is shown against the offset measured in the frame of the bar. The symbols have the same meaning as in Fig. 8.
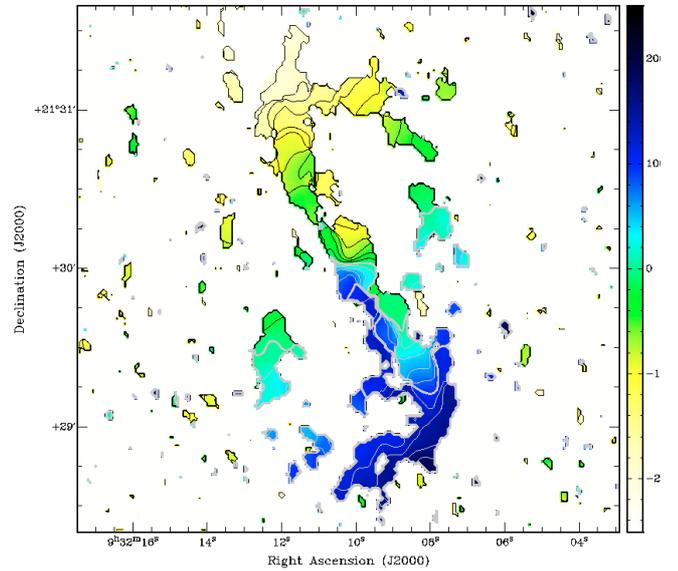

Fig. 11. The velocity field of the ^{12}CO(1–0) emission in NGC 2903 reproduced from the BIMA SONG survey by Helfer et al. (2003) shown as contours filled with color scale. The spatial resolution is 6.8″ × 5.5″. The levels of the velocity are from –200 to 200 km s^{-1} in steps of 20 km s^{-1}.

offset (–20, 0) where the velocity dispersion is 166 km s^{-1}. The ^{12}CO(1–0) map by Sheth et al. (2002) shows a CO complex slightly south of this position (C3 in their nomenclature) which contributes to the spread in velocity in the HCN(1–0) spectra.

The high velocity dispersion is likely due to beam smearing of large scale motion can be seen in the the BIMA-SONG ^{12}CO(1–0) high spatial resolution moment 1 map as shown in Fig. 11. The rotation curve shows an average velocity gradient of about 2.3 km s^{-1} arcsec^{-1}, which leads to about 60 km s^{-1} across the size of the HCN(1–0) beam, whereas the typical velocity dispersion for GMCs (Sanders et al. 1985) is only a few tens of km s^{-1}. This suggests that the higher velocity dispersion found along the bar is then likely due to streaming motion. The HCN(1–0) velocity dispersion in the leading edge of the bar is slightly higher than that of the bar axis, by about 10–20 km s^{-1}, except for the largest radius where the velocity dispersion is ~40 km s^{-1}. The rotation curve and the velocity dispersion measured using our low resolution HCN(1–0) observations is affected by the velocity gradients due to shock or streaming motion. A high spatial resolution observation would be

required to understand the role of shocks in the dynamics of the gas.

5. Star formation in the bar of NGC 2903

Comparison of the distribution of Hα emission with the ^{12}CO(1–0) emission by Sheth et al. (2002) suggests that the Hα emission is offset further toward the leading side of the ^{12}CO(1–0) emission, although a bright Hα complex is correlated with the peak ^{12}CO(1–0) emission on the northern side of the bar. On the trailing side of the bar only a few very diffuse Hα regions are detected. But this lack of HII regions cannot be explained by dust extinction as indicated by the low molecular gas surface density.

The lack of spatial resolution for the HCN(1–0) observations prevents precise comparison between the distribution of the Hα emission and the HCN(1–0) emission. However, detection of HCN(1–0) on the leading side of the bar, and the fact that the HCN(1–0) traces the dense molecular gas where SF activity is expected, indicate that the HCN(1–0) emission could be spatially correlated with the HII regions detected by Sheth et al. (2002).

The Hα data, kindly provided by Sheth (see Sheth et al. 2002, for more details), was calibrated using the scheme of Boselli & Gavazzi (2002) to obtain a total flux of 8.5×10^{-12} erg cm^{-2} s^{-1}. The Hα flux has to be corrected for dust extinction. This correction is rather uncertain since we do not know exactly the spatial distribution of dust in the Hα emitting region. An estimate of the extinction, A_V, from the molecular gas distribution (cf. Cernicharo & Guelin 1987) gives a value higher than 15 in the center. Alonso-Herrero et al. (2001) have estimated the A_V toward the center ranging from 1 to 6 mag using different optical tracers for the HII regions. We chose to take an average value of $A_V = 3$ mag in the center and $A_V = 1$ mag in the bar to correct the Hα flux. The Hα flux is uncertain within a factor of two because of the extinction and the NII line contribution (Martin & Friedli 1997).

Using the formula of Kennicutt (1989), the total SFR is estimated to be about ~1.4 $\mathcal{M}_\odot$ yr^{-1}. The SFR estimated over the HCN pointings is 0.36 $\mathcal{M}_\odot$ yr^{-1} in the bar and 0.67 $\mathcal{M}_\odot$ yr^{-1} in the center. The contrast in SFR between the center and the bar is 1.9. The central SFR is consistent with the estimate of Alonso-Herrero et al. (2001) but differs in the contrast found between the bar and the center by Knapen et al. (2002) because of a different extinction correction. We computed the SFR at each HCN offset position within the HCN IRAM-30 m beam. The local SFR in the center is about 15 to 150 times higher than that of the individual pointings in the bar. The SFR in the center is dominated by the known hot spots of recent star formation (Oka et al. 1974; Alonso-Herrero et al. 2001). The SFR at the HCN pointings in the bar are in the range ~0.01–0.05 $\mathcal{M}_\odot$ yr^{-1}. The SFR slowly decreases along the bar axis and the leading edge as shown in Fig. 12. But an inverse trend is present for the trailing edge of the bar where the SFR is lower in the inner positions (+10 and +30″) than that in the outer positions (+50 and +70″). These low values at the trailing edge of the bar are likely due to a low content of dense molecular gas and a low star formation efficiency. For the higher value at the end of the bar, a contribution from the star formation in the northern spiral arm which falls in the HCN beam cannot be ruled out.

The star formation efficiency can be estimated through the consumption time scale τ_{SF} of dense molecular gas, $M_{HCN}(H_2)/SFR$. In the center τ_{SF} is ~3×10^7 yrs, whereas in
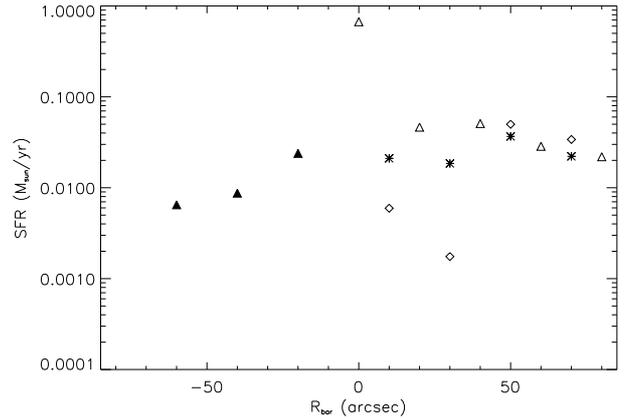

Fig. 12. The SFR, in $\mathcal{M}_\odot$ yr^{-1}, integrated over the IRAM-30 m beam at HCN(1–0) transition, shown against the offset measured in the axis of the frame. The symbols have same meaning as in Fig. 5. The SFR is taken above a threshold of 1.8×10^{-8} $\mathcal{M}_\odot$ yr^{-1} pc^{-2} (3σ).

the bar τ_{SF} ranges from 2 to 10 $\times 10^8$ yrs for the different positions. In the center, the short consumption time and the amount of dense molecular gas available for SF does not necessarily imply an earlier starvation of the inner starburst. The consumption time scale in the bar is much larger than the dynamical time for the inflow of gas to fuel the center (Friedli & Benz 1995; Martin & Friedli 1997). In addition, a much larger reservoir of molecular gas is available in the center.

6. Discussion

6.1. Ageing of the bar

Numerical simulations and observations of barred galaxies have shown that the SF and the distribution of the gas reveal a wide range of morphologies in the bar (Martin & Friedli 1997; Sheth et al. 2002; Verley et al. 2007). These different morphologies can be summarized into three different types, following Martin & Friedli (1997): (A) the galaxy exhibits SF along the bar without SF activity in the center; the duty cycle is relatively short, about 500 Myr or less; (B) SF activity is present along the bar and in the center of the galaxy. Simulations indicate that their duty cycle is variable ranging from 300 to 900 Myr. NGC 7479 is a typical example with intense SF along the bar and in the center (Zurita et al. 2001); (C) very little SF, or none at all, is present along the bar, whereas intense SF activity is present in the nuclear or circumnuclear region.

The ratio of SFR, β, between the center and the bar of NGC 2903 is 1.9. Comparison with the evolutionary path of β in a barred galaxy shown in Fig. 4 of Martin & Friedli (1997) suggests that NGC 2903 can be classified as a type B galaxy with a bar of age between 200 and 600 Myr. The age is dependent on the initial conditions in the disk of the galaxy (mass-to-gas ratio, mechanical energy released, SF, bulge mass). At the very early stages the models show that intense SF is visible along the leading edge of the bar, which indicates the presence of dense gas and is indeed observed in our HCN(1–0) data. Observations of newly born stars along the bar are consistent with the bar being young and the presence of Hα emission in the bar (Sheth et al. 2002) indicates that the bar can be rejuvenated by stars when a new supply of gas becomes available.

When the bar evolves, the SF decreases inside the bar and the β increases to typical values of about 20. The total lack of HCN(1–0) emission along the bar of NGC 3504 indicates that

this galaxy hosts a much older bar (type C), probably formed more than 1 Gyr ago (see Fig. 3 in Martin & Friedli 1997). The dense molecular gas reservoir available in the center of NGC 3504 is about ten times higher than that in NGC 2903 which should reach the same stage in a few hundred Myr.

6.2. Dense molecular gas

Detection of HCN(1–0) emission toward the center of galaxies is much more common in surveys of Seyfert galaxies (cf. Kohno et al. 2001; Huttemeister et al. 2000). However, very few barred galaxies have been mapped in the HCN(1–0) transition (Reynaud & Downes 1998; Huttemeister et al. 2000). We compare the gas properties of NGC 2903 with NGC 7479 and NGC 1530 which have been classified as type B barred galaxies (Martin & Friedli 1995). In NGC 7479 HCN(1–0) emission is seen only in the very center (Huttemeister et al. 2000). In NGC 1530, star formation is very intense around the nucleus and at the ends of the bar, whereas it is weak halfway between them but the shocks are more intense (Reynaud & Downes 1998). They concluded that the star formation may be inhibited by the strong shocks and the shear. In NGC 2903 the HCN(1–0) and the star formation do not show such a difference, HCN(1–0) is equally strong along the bar and the star formation does not exhibit a clear gradient toward the end, except at the center of the galaxy.

A striking feature of the current star formation is the strong curve shaped star formation region along the bar which indicates that SF may occur in dense molecular gas downstream of the shocked regions.

The galaxy, NGC 2903, currently appears to be a unique case of HCN(1–0) detection along its bar and at the center. The HCN(1–0) is distributed preferentially toward the leading edge of the bar. Most of the HII regions observed in the bar of NGC 2903 by Sheth et al. (2002) are downstream of the CO emitting regions. The association of the current star formation with dense molecular gas is a further indication that the HCN(1–0) is located downstream of the CO regions. The large velocity dispersion of the HCN(1–0) line indicates that the dense molecular gas may be located in regions with large velocity gradients, such as shocked regions. Shocks are expected to trace the dust lane in the bar (Athanassoula 1992). With the spatial resolution of the HCN(1–0) observations presented here, the location of the dense gas relative to the shocks cannot be established.

We also find an asymmetry in the line ratio, $\mathfrak{R}_{HCN/CO}$, and the SFR between the northern and the southern sides of the bar. The physical conditions and the dynamics of the dense molecular gas appear to be complex, and asymmetric along the bar. Higher spatial resolution observations of HCN(1–0) are necessary to clarify the situation.

7. Conclusion

We have mapped the HCN(1–0) emission along the bar of the spiral galaxies NGC 2903 and NGC 3504. From these observations we can draw the following conclusions:

– HCN(1–0) emission has been detected in the center of NGC 3504 and no emission is detected in the bar. The HCN(1–0) to ^{12}CO(1–0) line ratio is 0.12. The mass of the dense molecular gas in the center is $2.1 \times 10^8 \, \mathcal{M}_\odot$, which is about 15 % of the total mass of the molecular gas.
– In NGC 2903, HCN(1–0) emission was detected in the center and along the bar. The HCN(1–0) to ^{12}CO(1–0) line ratio

along the bar is found to vary from 0.07 to 0.12. This ratio is much lower in the center of the galaxy than in the bar on the northern side, suggesting that the fraction of dense gas in the bar is higher than that in the center. There is also an asymmetry in the HCN(1–0) emission between the northern and the southern side of the bar.
– The total dense molecular gas mass in the bar of NGC 2903 is $\sim 1.2 \times 10^8 \, \mathcal{M}_\odot$ which is about 6 times larger than the mass at the center of $\sim 2.2 \times 10^7 \mathcal{M}_\odot$. The HCN(1–0) emission is concentrated along the central axis and the leading edge of the bar. The fraction of dense molecular gas mass relative to the total molecular mass is higher along the leading edge of the bar (11%) than on the bar axis ($\sim$7%).
– The central velocity of HCN(1–0) emission is systematically lower by about 5 to 20 km s^{-1} in the leading edge of the bar than on the central axis of the bar. This drop is likely due to streaming motion along the bar. A large velocity dispersion of HCN(1–0) emission ranging from 40 to 170 km s^{-1} is observed along the bar. Comparison with the ^{12}CO(1–0) rotation curve suggests that this could be due to beam smearing of the rotational velocity over large scales, observed with a low spatial resolution.
– Intense SF activity seen in Hα is correlated with the dense molecular gas. The total star formation rate is estimated to be about 1.4 $\mathcal{M}_\odot$ yr^{-1}, with 0.67 $\mathcal{M}_\odot$ yr^{-1} in the center and 0.36 $\mathcal{M}_\odot$ yr^{-1} in the bar of NGC 2903. The consumption time of the dense molecular gas in the center of about 3 $\times$ 10^7 yrs is much shorter than that along the bar, ranging from 2 to 10 $\times$ 10^8 yrs. The dynamical time for the inflow of gas from the bar to the center is shorter than the consumption time scale suggesting that the inflow of the gas from the bar to the center will sustain SF activity in the center for a longer period.
– Comparison of the distribution of HCN(1–0) in the bars of NGC 3504 and NGC 2903 with the results from the numerical simulations of Martin & Friedli (1997) suggest that the bars of these galaxies are at different stages of evolution. The bar in NGC 3504 is of type C with age $\geq$1 Gyr, with most of the gas already in its center. NGC 2903 harbors a young type B bar with an age between 200 and 600 Myr, with a strong inflow of gas toward the center.

References

Aalto, S., Booth, R. S., Black, J. H., & Johansson, L. E. B. 1995, A&A, 300, 369
Alonso-Herrero, A., Ryder, S. D., & Knapen, J. H. 2001, MNRAS, 322, 757
Athanassoula, E. 1992, MNRAS, 259, 345
Boselli, A., & Gavazzi, G. 2002, A&A, 386, 124
Cernicharo, J., & Guelin, M. 1987, A&A, 176, 299
Combes, F., & Gerin, M. 1985, A&A, 150, 327
Downes, D., Reynaud, D., Solomon, P. M., & Radford, S. J. E. 1996, ApJ, 461, 186
Friedli, D., & Benz, W. 1995, A&A, 301, 649
Gao, Y., & Solomon, P. M. 2004, ApJS, 152, 63
Handa, T. Nakai, N. Sofue, Y. Hayashi, M., & Fujimoto, M. 1990, PASJ, 42, 1
Hatchell, J., Thompson, M. A., Millar, T. J., & MacDonald, G. H. 1998, A&AS, 133, 29
Helfer, T. T., & Blitz, L. 1993, ApJ, 419, 86

Helfer, T. T., Thornley, M. D., Regan, M. W., et al. 2003, ApJS, 145, 259

Huttemeister, S., Aalto, S., Das, M., & Wall, W. F. 2000, A&A, 363, 93

Jackson, J. M.; Eckart, A., Cameron, M., et al. 1991, ApJ, 375, 105

Kenney, J. D. P., & Young, J. S. 1989, ApJ, 344, 171

Kenney, J. D. P., Carlstrom, J. E., & Young, J. S. 1993, ApJ, 418, 687

Kennicutt, R. C. 1989, ApJ, 344, 685

Kennicutt, R. C. 1998, ARA&A, 36, 189

Knapen, J. H., Pérez-Ramí rez, D., & Laine, S. 2002, MNRAS, 337, 808

Kohno, K., Kawabe, R., & Vila-Vilaró, B. 1999a, Proceedings of the 3rd Cologne-Zermatt Symposium, The Physics and Chemistry of the Interstellar Medium

Kohno, K., Kawabe, R., & Vila-Vilaró, B. 1999b, ApJ, 511, 157

Kohno, K., Matsushita, S., & Vila-Vilaró, B. 2001, in The Central Kiloparsec of Starbursts and AGN: The La Palma Connection, ASP Conf. Proc. 249, ed. J. H. Knapen, J. E. Beckman, I. Shlosman, & T. J. Mahoney

Martin, P., & Friedli, D. 1997, A&A, 326, 449

Nguyen, Q.-R., Jackson, J. M., Henkel, C., Truong, B., & Mauersberger, R. 1992, ApJ, 399, 521

Oka, S., Wakamatsu, K., Sakka, K., Nishida, M., & Jugaku, J. 1974, PASJ, 26, 289O

Paglione, T. A. D., Tosaki, T., & Jackson, J. M. 1995, ApJ, 454, 117

Phillips, A.C 1993, A&AS, 183, 2306

Reynaud, D., & Downes, D. 1997, A&A, 319, 737

Reynaud, D., & Downes, D. 1998, A&A, 337, 671

Sanders, D. B., Scoville, N. Z., & Solomon, P. M. 1985, ApJ, 289, 373

Sheth, K., Vogel, S. N., & Harris, A. I. 2001, in Galaxy Disks and Disk Galaxies, ASP Conf. Ser., ed. J. G. Funes, S. J., & E. Maria Corsini

Sheth, K., Vogel, S. N., & Regan, M. W., et al. 2002, AJ, 124, 2581

Solomon, P. M., Downes, D., & Radford, S. J. E. 1992, ApJ, 387, 55

Telesco, C. M., & Harper, D. A. 1980, ApJ, 235, 392

Verley, S., Combes, F., Verdes-Montenegro, L., Bergond, G., & Leon, S. 2007, A&A, 474, 43

Young, J. S., & Scoville, N. 1982, ApJ, 260, 11

Young, J. S., & Devereux, N. A. 1991, ApJ, 373, 414

Young, J. S., Xie, S., Tacconi, L., et al. 1995, ApJS, 98, 219

Young, J. S., Allen, L. Kenney, J. D. P., Lesser, A., & Rownd, B. 1996, AJ, 112, 1903

Zurita, A., Rozas, M., & Beckman, J. E. 2001, Ap&SS, 276, 491